Theoretical Mechanistic Study on the Reaction of CN Radical with HNCN

ARTICLE *in* JOURNAL OF COMPUTATIONAL CHEMISTRY · MAY 2011

Impact Factor: 3.59 · DOI: 10.1002/jcc.21736 · Source: PubMed

4 AUTHORS, INCLUDING:

Chaozheng He
Nanyang Normal University
37 PUBLICATIONS **85** CITATIONS
SEE PROFILE

Jing-Yao Liu
Jilin University
148 PUBLICATIONS **736** CITATIONS
SEE PROFILE

Theoretical Mechanistic Study on the Reaction of CN Radical with HNCN

NAN-NAN WU, CHAO-ZHENG HE, XUE-MEI DUAN, JING-YAO LIU
Institute of Theoretical Chemistry, State Key Laboratory of Theoretical and Computational Chemistry, Jilin University, Changchun 130023, People's Republic of China

Received 31 May 2010; Revised 26 October 2010; Accepted 17 November 2010
DOI 10.1002/jcc.21736
Published online 24 January 2011 in Wiley Online Library (wileyonlinelibrary.com).

Abstract: The mechanism for the reaction of the cyanogen radical (CN) with the cyanomidyl radical (HNCN) has been investigated theoretically. The electronic structure information of the singlet and triplet potential energy surfaces (PESs) is obtained at the B3LYP/6-311+G(3df,2p) level, and the single-point energies are refined at the CCSD(T)/6-311+G(3df,2p) level as well as by multilevel MCG3-MPWB method. The calculations show that the C atom of CN additions to middle- and end-N atoms of HNCN are two barrierless association processes leading to the energy-rich intermediates IM1 HN(CN)CN and IM2 HNCNCN, respectively, on the singlet PES. The higher barriers of the subsequent isomerization and dissociation channels from IM1 and IM2 indicate that these two intermediates, which have considerably thermodynamic and kinetic stability, are the dominant product at high pressure. While at low pressure, the most favorable product is P_2 H + NCNCN, which will be formed from both IM1 and IM2 via direct dissociation processes by the H-N bond rupture, and the secondary feasible product is P_4 HCN + ^{1}NCN, while P_5 HCCN + N_2 and P_6 HCNC + N_2 are the least competitive products. On the triplet PES, P_{14} NCNC + HN may be a comparable competitive product at high temperature. In addition, the comparison between the mechanisms of the CN + HNCN and OH + HNCN reactions is made. The present results will enrich our understanding of the chemistry of the HNCN radical in combustion processes and interstellar space.

 J Comput Chem 32: 1449–1455, 2011

Key words: reaction mechanism; cyanogen radical (CN); cyanomidyl radical (HNCN); potential energy surface (PES); theoretical calculation

Introduction

The cyanomidyl radical (HNCN) is a reactive intermediate formed in the combustion of sulfur-containing fuels and plays an important role in combustion and interstellar processes due to its involvement in the "prompt" NO formation. The studies on spectroscopy and dynamics of the HNCN radical have been carried out experimentally.[1–5] Theoretically, *ab initio* calculations of the molecular structure and vibrational frequencies were performed by Tao et al.[6] and Puzzarini and Gambi.[7] Also, Lin and coworkers[8] first proposed the HNCN radical to be the key stable intermediate in the CH + N_2 reaction, which is important in hydrocarbon combustion, and Du and Zhang[9] reported that the HNCN radical is the major product in the association reaction of CN + NH_2.

Recently, some theoretical studies have been reported on the mechanisms of the OH + HNCN, $O(^3P)$ + HNCN, O_2 + HNCN and NO + HNCN reactions.[10–12] However, no kinetic studies have been performed on the reactivity of HNCN toward some important atmospheric species in experiment. It is known that the cyanogen radical (CN) is a very important radical in many environments ranging from astrophysics to combustion chemistry of nitrogen.[13–18] Both CN and HNCN may coexist in the interstellar and combustion space. The unpaired electrons of HNCN are likely to be stabilized by the CN radical, as a result, [HNCNCN] isomers or possible product fragments such as HCN and NCN, which are "prompt" NO precursors,[5,19–21] could be produced. However, to the best of our knowledge, no kinetic information of this reaction has been reported experimentally or theoretically. In view of the potential importance of both radi-

Correspondence to: J.-Y. Liu. e-mail: ljy121@jlu.edu.cn

Additional Supporting Information may be found in the online version of this article.

Contract/grant sponsor: National Natural Science Foundation of China; contract/grant numbers: 20303007, 20333050, 2097307

Contract/grant sponsor: Program for New Century Excellent Talents in University, China (NCET)

cals, a detailed theoretical investigation is very desirable to understand the relevance of HNCN in combustion and atmospheric chemistry. In this work, we carry out high-level *ab initio* calculations to gain a deep insight into the reaction mechanism and to determine the possible products of the CN + HNCN reaction. The information of both singlet and triplet potential energy surfaces (PESs) is obtained at the CCSD(T)/6-311+G(3df,2p)//B3LYP/6-311+G(3df,2p) level. In addition, the comparison between the CN + HNCN and OH + HNCN reactions is made.

Computational Method

The geometries of all of the reactants, products, intermediates, and transition states involved in the CN + HNCN reaction were optimized using hybrid density functional B3LYP[22,23] method in conjunction with the 6-311+G(3df,2p) basis set. Frequency calculations were performed at the same level to check whether the obtained species is an equilibrium species (with all real frequencies) or a transition state (with one and only one imaginary frequency). To confirm that the transition states connect designated intermediates, we also performed intrinsic reaction coordinate[24–27] calculations at the B3LYP/6-311+G(3df,2p) level. To obtain more reliable energetic data, single-point energy calculations were performed at the CCSD(T)/6-311+G(3df,2p) level using the B3LYP/6-311+G(3df,2p) optimized geometries of all the species. In addition, for the purpose of comparison, the single-point energies were calculated using one newly developed multilevel method MCG3-MPWB, which has proved to be one of the powerful methods for achieving higher-accuracy energies but with less computational cost.[28] Unless noted, the CCSD(T) energies with inclusion of B3LYP zero-point vibrational energies (ZPE) are used throughout. All calculations were carried out using the Gaussian 03 program packages.[29]

Results and Discussion

The schematic profiles of the singlet potential energy surface (PES) involving the energetically favorable and unfavorable reaction channels of the CN + HNCN reaction are depicted in Figures 1a and 1b, respectively, and the schematic profile of the triplet PES is shown in Figure 2. The optimized geometries of the relevant intermediates, transition states involved in the major reaction pathways and some low-lying isomers in the secondary reaction pathways on the PESs are also shown in Figures 1 and 2. For simplicity, the structures of the reactants as well as the most possible products are shown in Figure 3 along with the available experimental data from the literature. The optimized geometries of the other species are collected in the Supporting Information. It is seen that when comparison is available, the agreement between theoretical and experimental results is good, with the largest discrepancy within a factor of 0.9%. The total energy of the reactant **R** (CN + HNCN) is set to be zero for reference. There are 25 isomers, 55 transition states and 10 products involved in the singlet PES, while for the triplet PES, 12 isomers, 23 transition states and 8 products are found.

Singlet Potential-Energy Surface of CN + HNCN

There exist two resonance structures: HN=C=N ↔ HN≡C—N of the HNCN radical, thus the unpaired p electrons of the C atom of the CN radical may attack on either middle- or terminal-N atom of the HNCN radical, leading to the energy-rich entrance intermediate **IM1** HN(CN)CN (−93.9) or **IM2** HNCNCN (−96.4) on the singlet PES, respectively. The values in parentheses are the relative energies in kcal/mol with reference to **R**. Such radical–radical addition processes are barrierless. **IM1** and **IM2** can interconvert to each other by the 1, 3 H-shift transition state TS1 (−20.56). There are two dissociation pathways starting from **IM1** HN(CN)CN with C_{2V} symmetry: (1) H-extrusion of the H-N bond to form $\mathbf{P_2}$ NCNCN + H (−7.0) with no distinct barrier (see Fig. 1a); (2) via five-membered ring transition state TS37 (25.0) to form **IM20** (16.6) followed by the dissociation process to produce $\mathbf{P_6}$ HCNC + N_2 (−43.3) via TS38 (37.7) (see Fig. 1b). Although $\mathbf{P_6}$ has more thermodynamic stability, the formation of it from **IM1** is energetically unfeasible due to involving two high-lying transition states TS37 and TS38 in path (2).

Starting from **IM2** HNCNCN, there are five possible dissociation and isomerization pathways: (1) direct N-H bond rupture to give $\mathbf{P_2}$; (2) 1, 2 H-shift to form **IM7** (−40.3) via TS13 (−9.8); (3) 1, 2-migration of the CN group through TS2 (−2.5) to give **IM3** (−45.3); (4) concerted C—N bond rupture and N-N bond formation via three-membered ring transition state TS3 (−18.4) to form **IM4** (−49.9), and (5) via five-membered ring transition state TS4 (29.5) to form **IM5** (−49.5). Clearly, the formation of **IM5** is kinetically unfeasible, so for simplicity, herein further transformation and dissociation details from **IM5** in Figure 1b will not be discussed.

From Figure 1a, it is seen that isomer **IM7** can undergo a direct C-N bond fission to yield $\mathbf{P_4}$ HCN + ^{1}NCN (−14.3) via TS15 (−10.8). Alternatively, it can convert to isomer **IM8** (−20.8) via TS14 (−5.2), then **IM8** further isomerizes to a low-lying isomer **IM9** (−53.6) via TS16 (−1.6). Once isomer **IM9** is formed, four possible reaction pathways could take place, as shown in Figures 1a and 1b: (1) direct C—N bond rupture to produce product $\mathbf{P_6}$ HCNC + N_2 via TS17 (−35.0) (see Fig. 1a); (2) 1, 2-H-shift process to give $\mathbf{P_1}$ HNC + ^{1}CNN (23.7) via TS20 (28.0); (3) undergoing two sequential isomerization processes to form **IM11** (6.2) via TS18 (−27.9) and TS21 (26.3); (4) 1, 3-H-shift process to form isomer **IM12** (−24.5) through TS19 (38.8), followed by the C—N bond rupture leading to $\mathbf{P_6}$ via TS24 (−16.7). Since the transition states or fragment products in the latter three pathways paths (2) – (4) (see Fig. 1b) are energetic unfeasible, path (1) giving $\mathbf{P_6}$ is almost the exclusively feasible channel from **IM9**.

Isomer **IM3** can transform to other isomers **IM5**, **IM6** (−26.8), **IM13** (−8.9), **IM18** (−23.7) and **IM14** (−52.9) via TS5 (7.4), TS6 (8.0), TS25 (23.1), TS27 (40.7) and TS26 (−1.5), respectively. Seen from Figure 1b, the formations and further transformations of the former four intermediates are unlikely to occur due to the larger activated barriers required for achieving the interconversions. The only possible pathway is that **IM3** isomerizes to **IM14** after surmounting the barrier of 43.8 kcal/mol, and then **IM14** takes a 1, 3 H-shift via TS31

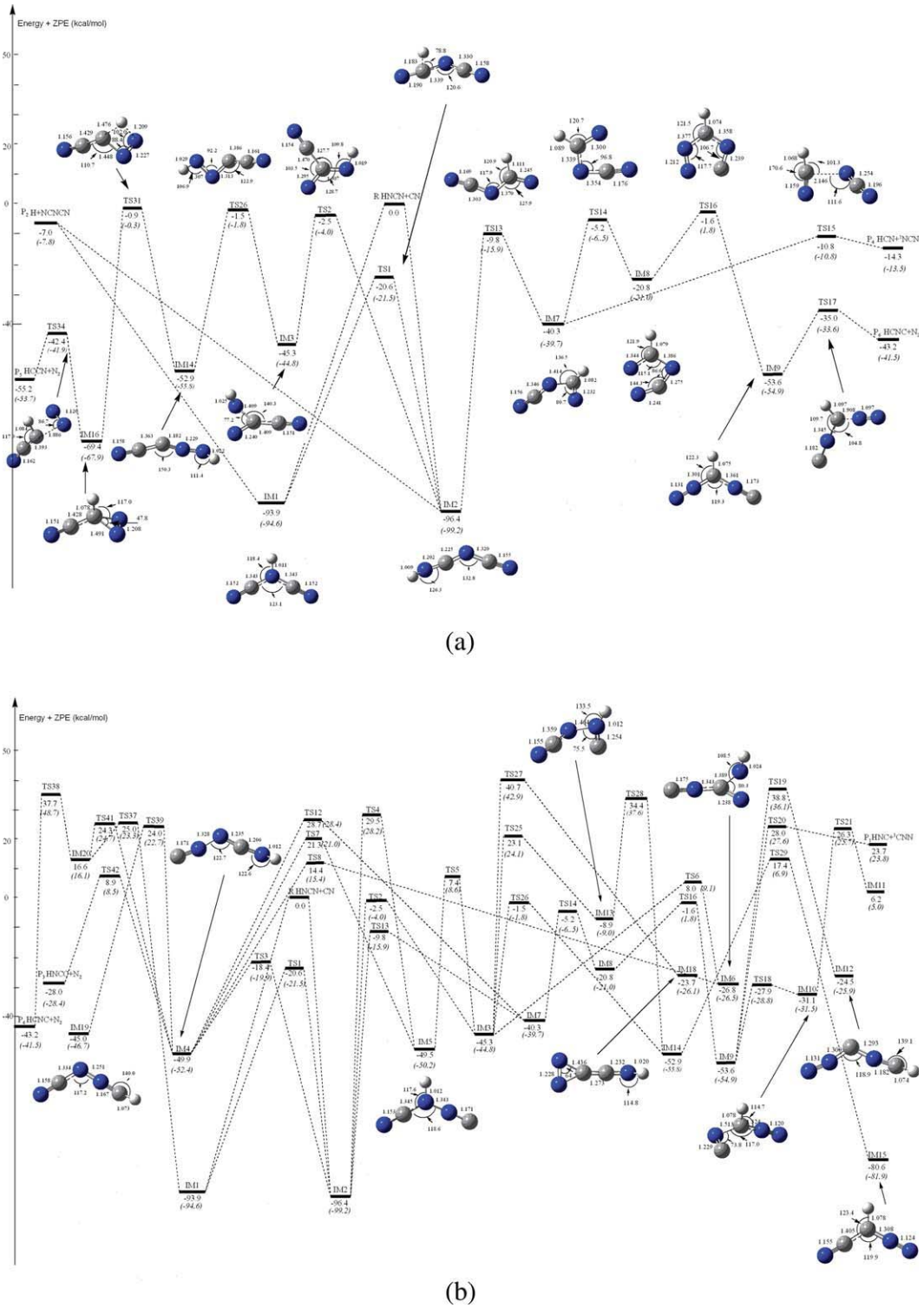

(a)

(b)

Figure 1. (a) Schematic singlet energy surface of the primary product channels for the CN + HNCN reaction at the CCSD(T)/6-311++G(d,p)//B3LYP/6-311+G(3d f,2p) + ZPE level. The italic values in parentheses are obtained at the MCG 3-MPWB//B3LYP + ZPE level. (b) Schematic singlet energy surface of the secondary product channels for the CN + HNCN reaction at the CCSD(T)/6-311++G(d,p)//B3LYP/6-311+G (3df,2p) + ZPE level. The italic values in parentheses are obtained at the MCG3-MPWB//B3LYP + ZPE level.

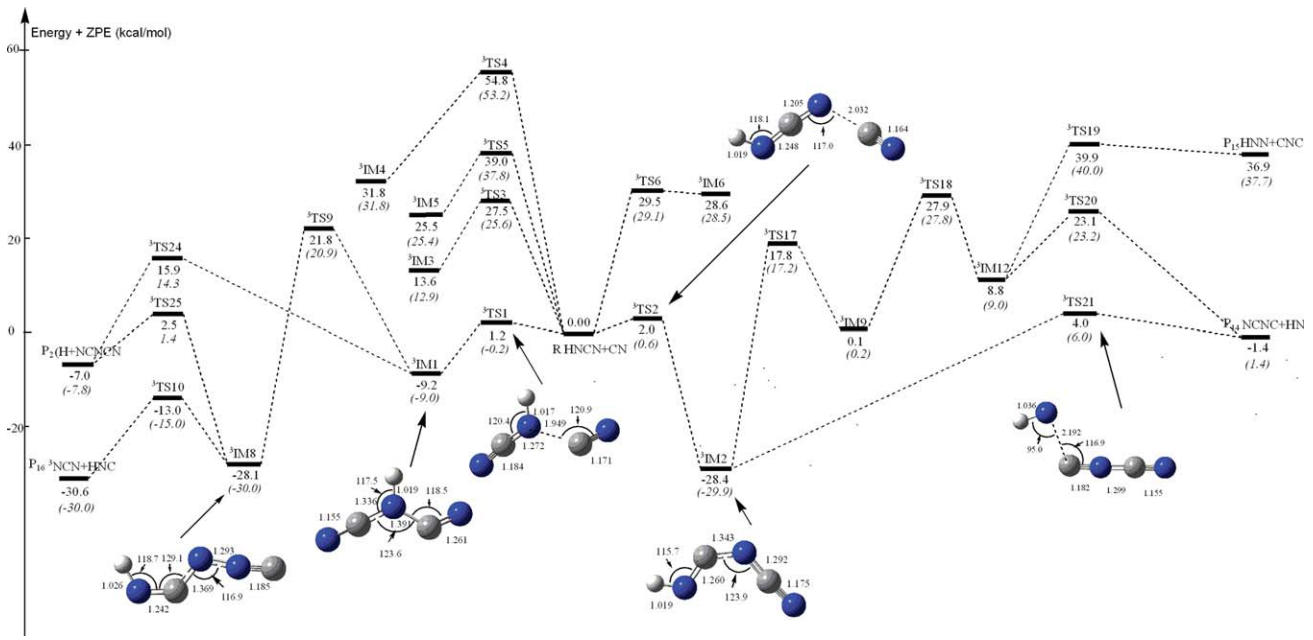

Figure 2. Schematic triplet energy surface of the reaction channels for the CN + HNCN reaction at the CCSD(T) /6-311++G(d,p)//B3LYP/6-311+G(3df,2p) + ZPE level. The italic values in parentheses are obtained at the MCG3- MPWB//B3LYP + ZPE level.

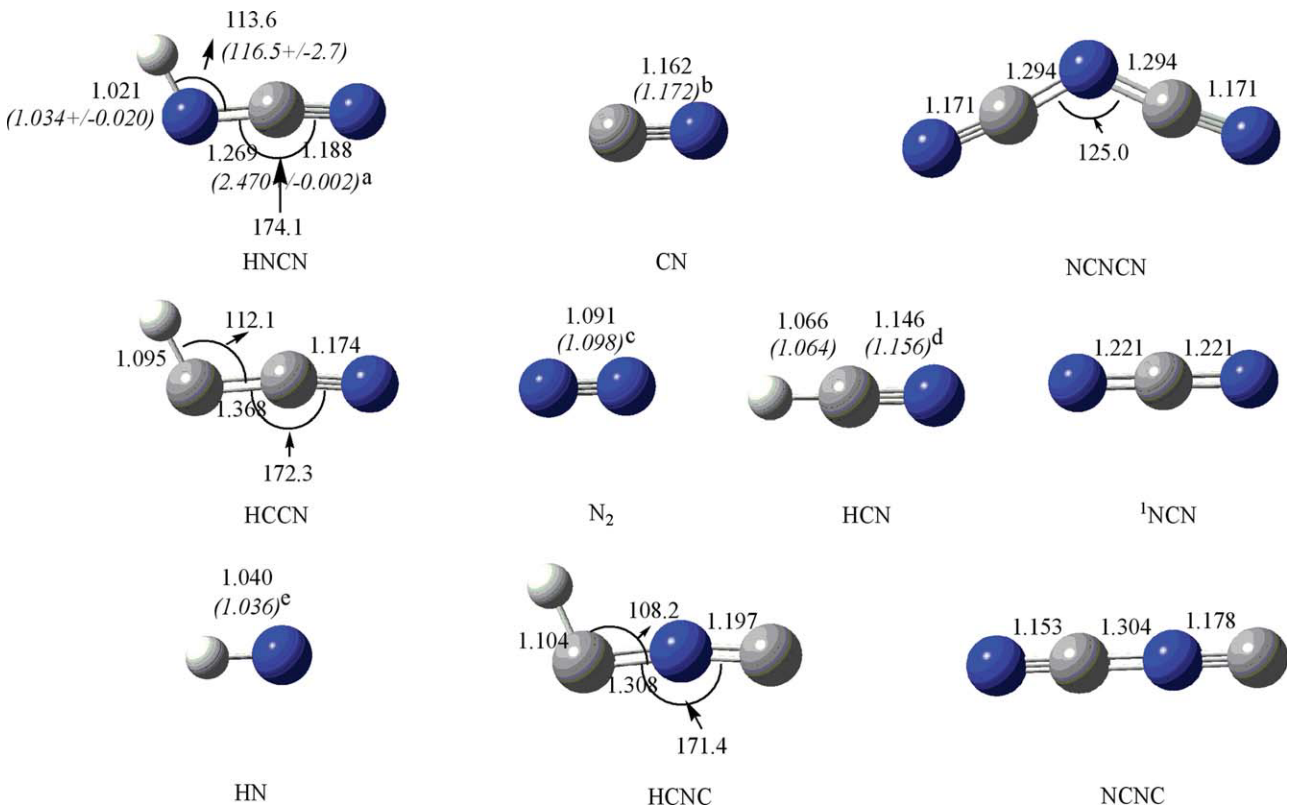

Figure 3. B3LYP/6-311+G(3df,2p) optimized geometries for the reactant as well as the most important products of the CN + HNCN reaction. The italic values in parentheses are the pertinent experimental data from the literature. Bond lengths are in angstroms and angles are in degrees. [a]Reference 1. [b,c,e]Reference 30. [d]Reference 31.

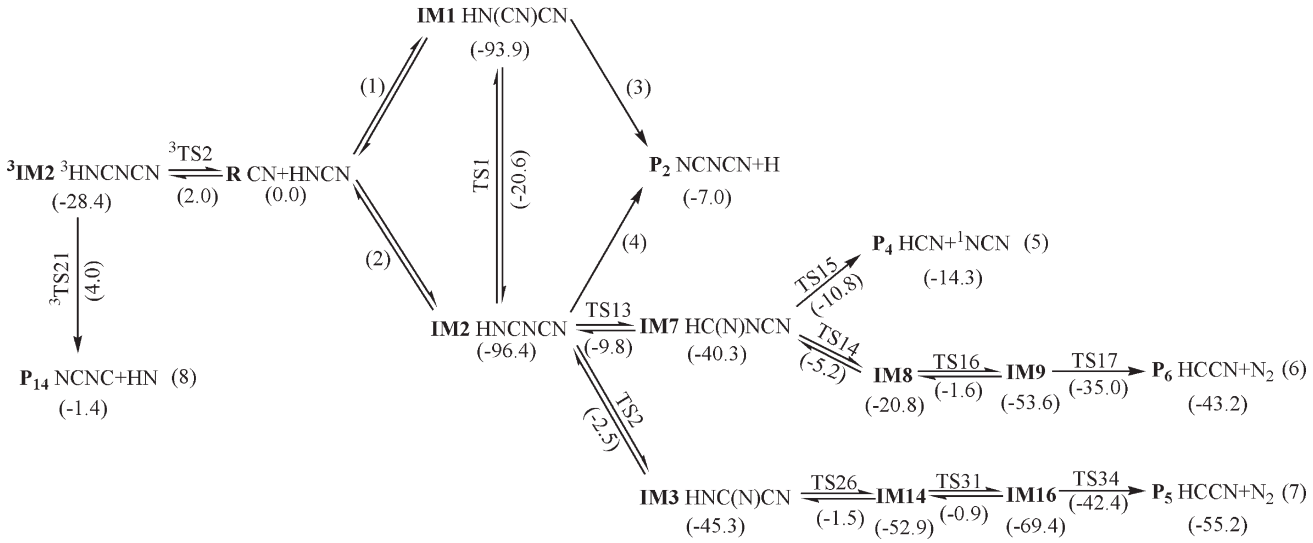

Scheme 1. The most possible reaction pathways on both singlet and triplet PESs for the reaction of CN + HNCN, where data in parentheses are relative energies in kcal/mol.

(−0.9) to form a three-membered ring low-lying isomer **IM16** (−69.4), followed by two concerted C—N bond ruptures to produce $\mathbf{P_5}$ HCCN + N_2 (−55.2) with a barrier of 27.0 kcal/mol.

Comparing with the above two isomerization processes from **IM2** as shown in Figure 1b, the interconversion from **IM2** to **IM4** has a relatively lower barrier (see Fig. 1b). However, it can hardly go through further transformations to form isomers **IM5**, **IM6**, **IM7**, **IM19** (−45.0), **IM20** (16.6) and product $\mathbf{P_3}$ HNCC + N_2 (−28.0) because of the higher barriers involved in these processes. The subsequent isomerization and dissociation processes from them are therefore unimportant for the title reaction.

Triplet Potential-Energy Surface of CN + HNCN

There are six entrance addition channels on the triplet PES. Unlike the association processes on the singlet PES, all of the attack channels are barrier-consumed processes. Both C and N atoms of the CN ($^2\sum$ radical may attack the middlel-N, termina-N and middle-C atoms of the HNCN radical, so six entrance intermediates ^{3}**IM1** ^{3}HN(CN)CN (−9.2), ^{3}**IM2** ^{3}HNCNCN (−28.4), ^{3}**IM3** ^{3}HNCNNC (13.6), ^{3}**IM4** ^{3}HN(CN)NC (31.8), ^{3}**IM5** ^{3}HNC(N)CN (25.5) and ^{3}**IM6** ^{3}HN(CN)NC (28.6) are located via transition states ^{3}TS1 (1.2), ^{3}TS2 (2.0), ^{3}TS3 (27.5), ^{3}TS4 (54.8), ^{3}TS5 (39.0), and ^{3}TS6 (29.5), respectively. Because isomers ^{3}**IM3** – ^{3}**IM6** as well as their associated transition states lie much higher than the reactants, the formation of ^{3}**IM3** – ^{3}**IM6** are both thermodynamically and kinetically prohibited, and also their further transformations are negligible. The attack of the C atom of CN at the middle-N atom of HNCN overcomes a barrier of 1.2 kcal/mol to form a relatively shallow intermediate ^{3}**IM1**, which takes successive isomerization and dissociation pathways to yield $\mathbf{P_{16}}$ ^{3}NCN + HNC (−30.6). Such process needs to pass through two transition states ^{3}TS9 (21.8) and ^{3}TS10 (−14.3) via an intermediate ^{3}**IM8** (−28.1). Since ^{3}TS9 is much higher than **R**, the formation pathway of product $\mathbf{P_{16}}$ is kinetically inaccessible. A barrier of 2.0 kcal/mol for the C-attack of CN at the end-N site of HNCN is required to form intermediate ^{3}**IM2**. Subsequently, ^{3}**IM2** favorably undergoes a C—N bond rupture to produce product $\mathbf{P_{14}}$ NCNC + HN (−1.4) via ^{3}TS21 (4.0). Thus, this channel is the most favorable channel on the triplet PES.

Reaction Mechanism and Implications

In summary, the most possible reaction pathways (see Figs. 1a and 2) on both singlet and triplet PESs for the reaction of CN + HNCN at the CCSD(T)//B3LYP level are depicted in Scheme 1. It is seen that, on the singlet PES, the barrierless addition processes of the two radicals lead to two energized HNCNCN intermediates **IM1** and **IM2**, with binding energies of 93.9 and 96.4 kcal/mol, respectively. The released rather large heat makes further isomerization or dissociation from them possible. **IM1** and **IM2** can interconvert to each other via a low-lying transition state TS1 (−20.6 kcal/mol), and both of them may undergo a direct N-H bond rupture to form product $\mathbf{P_2}$. Moreover, **IM2** is the gateway not only to $\mathbf{P_2}$ but also to the two lower-lying intermediates **IM3** and **IM7**, which can take successive transformations to yield three products $\mathbf{P_4}$, $\mathbf{P_5}$ and $\mathbf{P_6}$. As can be seen from Scheme 1, the rate-determining transition states TS16 (−1.62 kcal/mol) in **Path 6** and TS31 (−0.88 kcal/mol) in **Path 7** lie much higher than TS13 (−9.78) in **Path 5** and $\mathbf{P_2}$ in **Path 4**, and the formations of $\mathbf{P_5}$ and $\mathbf{P_6}$ need more steps than those of $\mathbf{P_2}$ and $\mathbf{P_4}$, consequently, the former two pathways **Path 6** and **Path 7** may be the least competitive channels, and $\mathbf{P_5}$ and $\mathbf{P_6}$, though with more thermodynamic stability, will be much difficult to be formed. In addition, although $\mathbf{P_2}$ lies slightly higher than the rate-determining transition state TS13 in **Path 5** by 2.8 kcal/mol, the formation of $\mathbf{P_2}$, which is a direct N-H bond rupture via a loose transition state from both early wells **IM1** and **IM2**, is simpler and more feasible than the formation of $\mathbf{P_4}$, which undergoes two steps via two tight transition states TS13 and TS15 (−10.8). Thus, $\mathbf{P_2}$ could be the most favorable prod-

uct for the reaction and **P_4** is in the secondary. On the triplet PES **Path 8** proceeds via addition-elimination mechanism to produce **P_{14}**. Due to the energy of the rate-determining transition state ^{3}TS21 only above the reactants by 4.0 kcal/mol, this relatively simple pathway may become a comparable competitive pathway at high temperature. Therefore, without performing further kinetic calculations to obtain the branching ratios of various isomers or products, just from the energetic point of view, we may qualitatively predict that under the condition with very low pressure (collisional stabilization effect can be neglected), **P_2** H + NCNCN may be the major product, and **P_4** HCN + ^{1}NCN may be secondary one with a comparable yield, while **P_5** HCCN + N_2 and **P_6** HCNC + N_2 should be the least products; moreover, at high temperature, the product channel leading to **P_{14}** NCNC + HN would become feasible in combustion. While under the condition with high pressure, **IM1** and **IM2**, with higher thermodynamic and kinetic stability, are the dominant products.

Also, it is worthwhile to make a comparison between the results obtained by different levels or methods. As is well known that the couple cluster technique with large basis set could provide accurate energies in most cases, while such calculations are much computationally demanding and thus unavailable especially for larger systems. In recent years, different multilevel techniques such as Gaussian-x[32–34] series and multicoefficient correlation methods[35–42] have been developed and widely applied in many studies. Recently, one newly developed multilevel method MCG3-MPWB[28] has been asserted to be a powerful method for calculating high-accuracy thermochemistry and potential energy surface features such as saddle point energies but with less expense. To test the accuracy and efficiency of this method, the single-point energy calculations for all the stationary points of the title reaction are also done by the MCG3-MPWB method. The MCG3-MPWB results (the italic values in parentheses) are given in Figures 1 and 2 for comparison. It is seen that in most cases, the agreement of the MCG3-MPWB energies with the CCSD(T) ones is good; the discrepancies are usually found to be within 3 kcal/mol. More importantly, such discrepancies do not affect the discussions on the reaction mechanism. Both CCSD(T) and MCG3-MPWB methods predict the same overall reaction mechanism and identify the same major products. The present results indicate that, in comparison with the "golden standard" CCSD(T) method, which is computationally expensive, the alternative multilevel MCG3-MPWB method offers an acceptable compromise between computational accuracy and cost. Therefore, the MCG3-MPWB method is particularly highly recommended when the CCSD(T) calculations become unaffordable especially for larger systems.

Moreover, it is very interesting to compare the present results with the recent theoretical investigation on the OH + HNCN reaction.[10] The initial association ways are both barrierless, leading to the thermodynamically stable intermediates HON(H)CN (46.9 or 44.2 kcal/mol) and HONCNH (41.4 kcal/mol) in the OH + HNCN reaction and HN(CN)CN (93.9 kcal/mol) and HNCNCN (96.4 kcal/mol) in the CN + HNCN reaction. Yet, the major products and the formation processes quite differ for both reactions. For the OH + HNCN reaction, NCN radical and H_2O molecule as the primary products are produced on both the singlet and triplet PESs, whereas for the CN + HNCN reaction, different feasible products are yielded on the singlet and triplet PESs, respectively. On the singlet PES, NCNCN + H is the most favorable product formed via the direct dissociations from above two intermediates, while the formation of the fragment NCN via the addition-elimination mechanism is the secondary pathway; on the triplet PES, product NCNC + HN is the major one and may occupy a comparable part only at high temperature. In addition, given the initial association energies of the entrance intermediates formed in the two reactions, it is reasonable to expect that the association process of CN + HNCN may be much faster than that of OH + HNCN. Meanwhile, the higher kinetic and thermodynamic stability of **IM1** and **IM2** as discussed above indicates that these two intermediates could exist and may be detected by future experiments. Therefore, it is reasonable to predict that the reaction of HNCN + CN may play an important role in interstellar and combustion processes similar to the reaction of HNCN with OH.

Conclusion

Detailed singlet and triplet PESs of the CN + HNCN reaction have been investigated at the B3LYP/6-311+G(3df,2p) and CCSD(T)/6-311+G(3df,2p) (single-point) levels. This reaction prefers to occur on the singlet surface. The initial association ways are the barrierless C-attack of CN at the middle- and end-N atom of HNCN leading to low-lying intermediates **IM1** HN(CN)CN and **IM2** HNCNCN. From **IM1** and **IM2**, the primary product is **P_2** H + NCNCN, which can be formed directly via the N-H bond rupture with no distinct barrier, and **P_4** HCN + ^{1}NCN is the secondary product; **P_5** HCCN + N_2 and **P_6** HCNC + N_2 are the least feasible products, though with more thermodynamic stability, the rate-determining transition states in their formation channels are much higher in energy than those of **P_2** and **P_4**. Also, the triplet-surface product **P_{14}** NCNC + HN may have a comparable contribution to the final product distribution at high temperature. Moreover, the single-point energies, which are obtained by the multilevel MCG3-MPWB method with much less computationally expensive show reasonable agreement with the CCSD(T)/6-311+G(3df,2p) results. The comparison between the CN + HNCN and OH + HNCN reactions indicates that the reaction under study may play an important role in interstellar and combustion processes. This study may be useful for deeply understanding the mechanism and future experimental identification of the product distributions for the CN + HNCN reaction.

Acknowledgments

The authors are grateful to the referees for their valuable comments on improving the manuscript.

References

1. Herzberg, G.; Travis, D. N. Can J Phys 1963, 41, 286.
2. Wu, M.; Hall, G.; Sears, T. J. J Chem Soc Faraday Trans 1993, 89, 615.

3. Yamamoto, S.; Saito, S. J Chem Phys 1994, 101, 10350.
4. Clifford, E. P.; Wenthold, P. G.; Lineberger, W. C.; Petersson, G.; Ellison, G. B. J Phys Chem A 1997, 101, 4338.
5. Bise, R. T.; Hoops, A. A.; Neumark, D. M. J Chem Phys 2001, 114, 9000.
6. Tao, F.-M.; Klemperer, W.; Thaddeus, P. J Chem Phys 1994, 100, 3691.
7. Puzzarini, C.; Gambi, A. J Chem Phys 2005, 122, 064316.
8. Moskaleva, L. V.; Xia, W. S.; Lin, M. C. Chem Phys Lett 2000, 331, 269.
9. Du, B.; Zhang, W. C. Int J Quantum Chem 2006, 106, 1827.
10. Xu, S. C.; Lin, M. C. J Phys Chem A 2007, 111, 6730.
11. Xu, S. C.; Lin, M. C. Proc Combust Inst 2009, 32, 99.
12. Jian, R. C.; Tsai, C.; Hsu, L. C.; Chen, H. L. J Phys Chem A 2010, 114, 4655.
13. Haynes, B. S.; Iverach, D.; Kirov, N. Y. Fifteenth Symposium (International) on Combustion; The Combustion Institute: Pittsburgh, 1974; p. 1103.
14. Albers, E. A.; Hoyermann, K.; Schake, H.; Schmatijko, K. J.; Wagner, H. Gg.; Wolfrum, J. Fifteenth Symposium (International) on Combustion; The Combustion Institute: Pittsburgh, 1974; p. 765.
15. Haynes, B. S. Combust Flame 1977, 28, 113.
16. Miller, J. A.; Branch, M. C.; Mclean, W. J.; Chandler, D. W.; Smooke, M. D.; Kee, R. J. Twentieth Symposium (International) on Combustion; The Combustion Institute: Pittsburgh, 1984; p. 673.
17. Bauschlicher, C. W.; Langhoff, S. R.; Taylor, P. R. AstrophysJ 1988, 332, 531.
18. Thorne, L. R.; Branch, M. C.; Chandler, D. W.; Kee R. J.; Miller, J. A. Symp Int Combust Proc 1986, 21, 965.
19. Berman, M. R.; Lin. M. C. J Phys Chem 1983, 87, 3933.
20. Miller, J. A.; Walch, S. P. Int J Chem Kinet 1997, 29, 253.
21. Cui, Q.; Morokuma, K. Theor Chem Acc 1999, 102, 127.
22. Becke, A. D. J Chem Phys 1993, 98, 5648.
23. Stevens, P. J.; Devlin, F. J.; Chablowski, C. F.; Frisch, M. J. J Phys Chem 1994, 98, 11623.
24. Fukui, K. Acc Chem Res 1981, 14, 363.
25. Page, M.; Mclver, J. W., Jr. J Chem Phys 1988, 88, 922.
26. Gonzalez, C.; Schlegel, H. B. J Chem Phys 1989, 90, 2154.
27. Gonzalez, C.; Schlegel, H. B. J Phys Chem 1990, 94, 5523.
28. Zhao, Y.; Lynch, B. J.; Truhlar, D. G. Phys Chem Chem Phys 2005, 7, 43.
29. Frisch, M. J.; Truck, G. W.; Schlegel, H. B.; Scuseria, G. E.; Robb, M. A.; Cheeseman, J. R.; Zakrzewski, V. G.; Montgomery, J. A., Jr.; Stratmann, R. E.; Burant, J. C.; Dapprich, S.; Millam, J. M.; Daniels, A. D.; Kudin, K. N.; Strain, M. C.; Farkas, O.; Tomasi, J.; Barone, V.; Cossi, M.; Cammi, R.; Mennucci, B.; Pomelli, C.; Adamo, C.; Clifford, S.; Ochterski, J.; Petersson, G. A.; Ayala, P. Y.; Cui, Q.; Morokuma, K.; Malick, D. K.; Rabuck, A. D.; Raghavachari, K.; Foresman, J. B.; Cioslowski, J.; Ortiz, J. V.; Boboul, A. G.; Stefnov, B. B.; Liu, G.; Liaschenko, A.; Piskorz, P.; Komaromi, L.; Gomperts, R.; Martin, R. L.; Fox, D. J.; Keith, T.; Al–Laham, M. A.; Peng, C. Y.; Nanayakkara, A.; Gonzalez, C.; Challacombe, M.; Gill, P. M. W.; Johnson, B.; Chen, W.; Wong, M. W.; Andres, J. L.; Gonzalez, C.; Head–Gordon, M.; Replogle E. S.; Pople, J. A. Gaussian 03, Revision A.1, Guassian, Inc., Pittsburgh, PA, 2003.
30. Huber, K. P.; Herzberg, G. Molecular Spectra and Molecular Structure. IV. Constants of Diatomic Molecules, Van Nostrand Reinhold, New York, 1979.
31. Herzberg, G., Electronic Spectra and Electronic Structure of Polyatomic Molecules, Van Nostrand Reinhold, New York, 1966.
32. Curtiss, L. A.; Raghavachari, K.; Redfern, P. C.; Rasslov, V.; Pople, J. A. J Chem Phys 1991, 94, 7221.
33. Curtiss, L. A.; Raghavachari, K.; Redfern, P. C.; Rasslov, V.; Pople, J. A. J Chem Phys 1998, 109, 7764.
34. Curtiss, L. A.; Redfern, P. C.; Raghavachari, K. J Chem Phys 2007, 126, 84108.
35. Fast, P. L.; Corchado, J.; Sanchez, M. L.; Truhlar, D. G. J Phys Chem A 1999, 103, 3139.
36. Fast, P. L.; Corchado, J.; Sanchez, M. L.; Truhlar, D. G. J Phys Chem A 1999, 103, 5129.
37. Fast, P. L.; Corchado, J.; Sanchez, M. L.; Truhlar, D. G. J Chem Phys 1999, 110, 11679.
38. Fast, P. L.; Sanchez, M. L.; Truhlar, D. G. Chem Phys Lett 1999, 306, 407.
39. Tratz, C. M.; Fast, P. L.; Truhlar, D. G. PhysChemComm 1999, 2, 14.
40. Fast, P. L.; Truhlar, D. G. J Phys Chem A 2000, 104, 6111.
41. Lynch, B. J.; Truhlar, D. G. J Phys Chem A 2002, 106, 842.
42. Lynch, B. J.; Truhlar, D. G. J Phys Chem A 2003, 107, 3898.